Biochimica et Biophysica Acta, 513 (1978) 43—58

BBA 78162

THE EFFECT OF CHOLESTEROL ON THE STRUCTURE OF PHOSPHATIDYLCHOLINE BILAYERS

THOMAS J. McINTOSH

Department of Anatomy, Duke University School of Medicine, Durham, N.C. 27710 (U.S.A.)

(Received March 13th, 1978)

Summary

The effect of cholesterol on the structure of phosphatidylcholine bilayers was investigated by X-ray diffraction methods. Electron density profiles at 5 Å resolution along with chain tilt and chain packing parameters were obtained and compared for phosphatidylcholine/cholesterol bilayers and for pure phosphatidylcholine bilayers in both the gel and liquid crystalline states. The cholesterol in the bilayer was localized by noting the position of discrete elevations in the electron density profiles. Cholesterol can either increase or decrease the width of the bilayer depending on the physical state and chain length of the lipid before the introduction of cholesterol. For saturated phosphatidylcholines containing 12—16 carbons per chain, cholesterol increases the width of the bilayer as it removes the chain tilt from gel state lipids or increases the trans conformations of the chains for liquid crystalline lipids. However, cholesterol reduces the width of 18 carbon chain bilayers below the phase transition temperature as the long phospholipid chains must deform or kink to accomodate the significantly shorter cholesterol molecule. Although cholesterol has a marked effect on hydrocarbon chain organization, it was found that, within the resolution limits of the data, the phosphatidylcholine head group conformation is unchanged by the addition of cholesterol to the bilayer. The head group is oriented parallel to the plane of the bilayer for phosphatidylcholine in the gel and liquid crystalline states and this orientation is not changed by the addition of cholesterol.

Introduction

Phosphatidylcholine/cholesterol bilayers have been studied extensively because of their relevance to biological membranes. The effect of cholesterol

Abbreviations: DLPC, dilauryl phosphatidylcholine; DMPC, dimyristoyl phosphatidylcholine; DPPC, dipalmitoyl phosphatidylcholine; DSPC, distearoyl phosphatidylcholine.

on phosphatidylcholine bilayers has been analyzed by a number of techniques, including monolayer surface chemistry [1,2], Raman spectroscopy [3], calorimetry [4], nuclear magnetic resource [5,6], electron spin resource [7,8], neutron diffraction [9], and X-ray diffraction [10—12]. In particular, X-ray diffraction data have given valuable information on the effect of cholesterol on lipid hydrocarbon chain organization [4,11]. In terms of high resolution (5 Å or better) X-ray structural studies, Blasie and colleagues [13,14] have analyzed synthetic dipalmitoyl phosphaditylcholine below the lipid phase transition temperature and Franks [15] has analyzed egg phosphatidylcholine/cholesterol bilayers at temperatures above the phase transition of egg phosphatidylcholine. Since these latter two studies were made using different lipids under different conditions it is difficult to compare directly the two results to determine the modification of bilayer organization caused by cholesterol. In order to get as much information as possible from the X-ray technique, this study compares electron density profiles and hydrocarbon chain packing parameters for highly oriented bilayers of chemically well-defined synthetic phosphatidylcholine, both in the gel and liquid crystalline states, and for the same lipids with added cholesterol. This current paper will deal with the localization and structural effects of cholesterol in saturated phosphatidylcholines. Of particular interest is the manner in which phosphatidylcholines varying in chain length from 12 to 18 carbons can accomodate the bulky cholesterol molecule. A future paper (McIntosh, T.J., manuscript in preparation) will analyze the structure of chemically well-defined unsaturated phosphatidylcholine bilayers with and without incorporated cholesterol.

Materials and Methods

Saturated, synthetic L-α-phosphatidylcholines with hydrocarbon chains containing 12 (dilauryl), 14 (dimyristoyl), 16 (dipalmitoyl), and 18 carbons (distearoyl) were obtained from Calbiochem or Applied Science. Cholesterol was purchased from Sigma Chemical Co. All lipids were used without further purification, and the same lipids from different commercial sources gave identical diffraction patterns. 2 : 1 molar ratios of phosphatidylcholine to cholesterol were used in these experiments as it has been shown that a stable complex forms at this molar ratio [6,16—18].

Oriented multilayer specimens were obtained either by slow evaporation of aqueous suspensions of the lipid in a constant humidity chamber or by a direct evaporation of mixtures of lipid and various organic solvents under a gentle stream of nitrogen [15]. Both of these methods gave diffraction patterns with the same repeat periods and intensity distributions. However, the best orientation and resolution was obtained when the lipids were deposited onto thin glass plates from ethanol above the lipid's phase transition temperature in a manner similar to that described by Birrell and Griffith [19]. The multilayers on the supporting plate were oriented in a Unican oscillation camera so that the planes of the bilayers were approximately parallel to a pinhole collimator. The specimen was oscillated through an appropriate angle so that diffraction orders out to 1/3 $Å^{-1}$ in reciprocal space could be recorded. To record wide-angle reflections from the lipid hydrocarbon chains the sample was held stationary or

oscillated through a smaller angle. Either a rotating anode X-ray generator designed by Dr. William Longley of this laboratory [20] or a stationary anode Jarrel-Ash generator was used to produce copper Kα X-radiation. A pinhole collimator and a nickel filter were used with a flat plate film cassette loaded with three or more sheets of Ilford Industrial G X-ray Film. Specimen-to-film distances were between 4 and 8 cm and exposure times were from 1 to 5 h.

Diffraction data were processed by standard methods. The discrete lamellar low-angle reflections obeyed Bragg's law: $2d \sin\Theta = h\lambda$, where d is the repeat period, Θ is the Bragg angle, h is the number of the diffraction order, and λ is the wavelength of the incident radiation. Densitometer traces were recorded on a Joyce-Loebl microdensitometer model MKIIIC, the background curve was subtracted, and integrated intensities $I(h)$ were measured. The standard Lorentz-polarization factor for oscillation photographs was used [21] and structure amplitudes $|T(h)| = \sqrt{hI(h)}$ were obtained. Electron density profiles, $\rho(x)$, were calculated by use of the formula $\rho(x) \propto \Sigma_h |T(h)| \phi(h) \cos(2\pi h/d)$ where $\phi(h)$ is the phase for each order h, and must be either + or − for a centrosymmetric system. The determination of $\phi(h)$ is discussed in Results. All profiles are on relative electron density scales.

The temperature and relative humidity at the specimen were controlled by use of a special chamber designed by Dr. M.J. Costello of this laboratory. The closed chamber contained mylar windows for the X-ray beam, a heating element, a thermocouple to monitor temperature at the specimen, and reservoir where various salt solutions were placed to adjust the relative humidity within the chamber [22]. By changing the relative humidity, the water content of the lipid multilayers could be varied between approx. 5 and 20% [9,11].

Results

For all specimens, the lamellar diffraction patterns consist of discrete Bragg reflections to between 1/6 and 1/4 $Å^{-1}$ in reciprocal space. Typical lamellar patterns for DLPC and DLPC/cholesterol multilayers are shown in Figs. 1A and 1B. Note the sharpness of the spots and the small mosaic spread present. The high degree of orientation makes it possible to obtain directly chain tilt information from the wide-angle patterns. The spacing and orientation of the wide-angle reflections depend on the physical state and degree of hydration of the lipid, as shown in Figs. 1C, 1D, and 1E. For pure phosphatidylcholine bilayers in the gel state, the patterns contain sharp reflections at a spacing of 4.2 Å. The orientation of these spots changes with increasing hydration of the pure phospholipid bilayers. When the phosphatidylcholine multilayers are in low (40%) relative humidity atmosphere the sharp 4.2 Å reflections are located directly on on the equator of the X-ray film, as in Fig. 1C. This indicates that the hydrocarbon chains are oriented perpendicular to the plane of the bilayer. At higher relative humidities, the lipid becomes more hydrated and sharp diffraction spots at 4.2 Å appear at an angle to the equator of the X-ray film (Fig. 1D). Levine [23] interpreted patterns like these in terms of chain tilt of the lipids, with the maximum chain tilt being about 30° from the normal to the plane of the bilayer when the phosphatidylcholine multilayers contain 20% water or more.

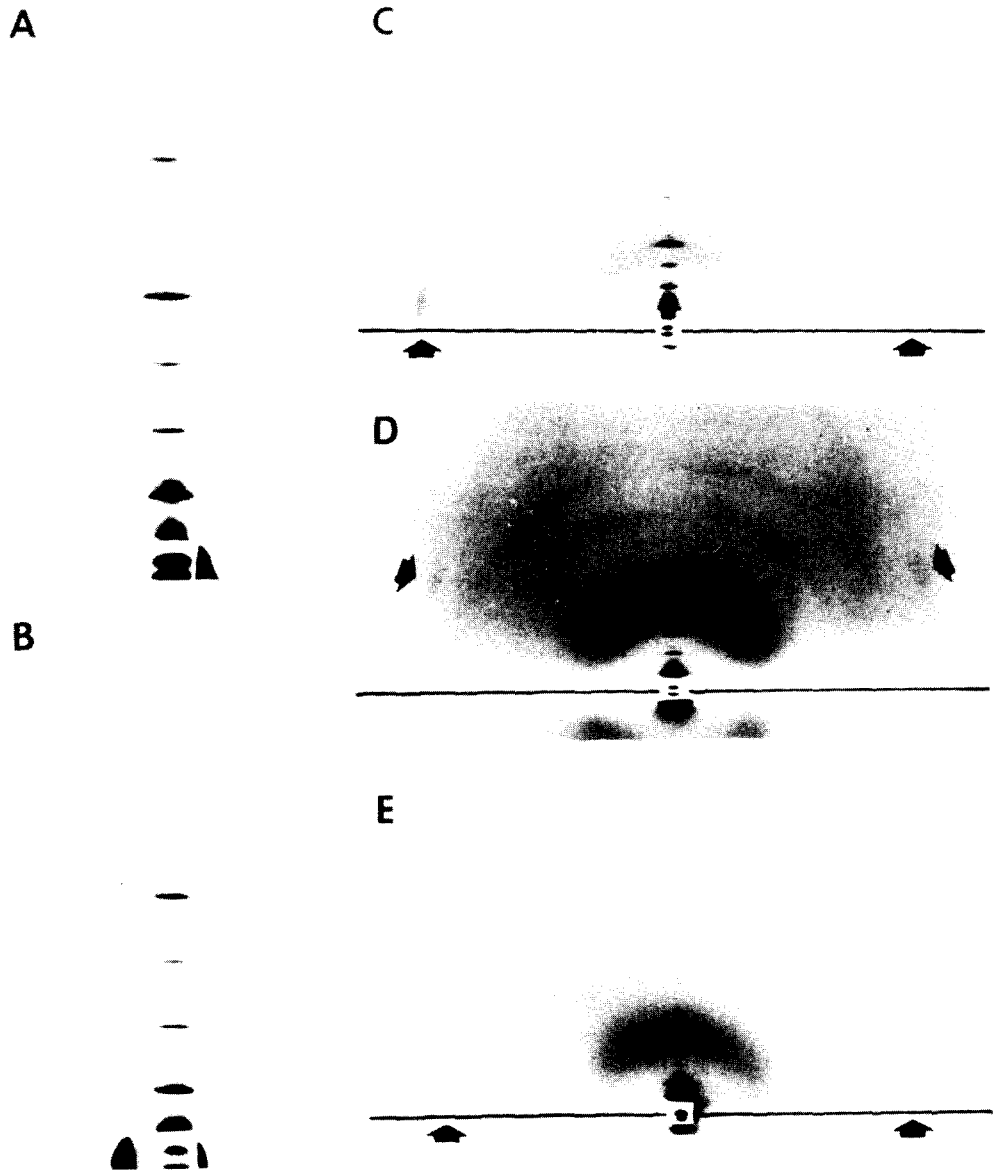

Fig. 1. Typical lamellar, low-angle (A, B) and wide-angle (C, D, E) diffraction patterns from oriented phosphatidylcholine and phosphatidylcholine/cholesterol multilayers. One half of each diffraction pattern is shown and a narrow black line has been drawn in on the equator at the bottom of the wide-angle patterns. The low-angle patterns have been photographically enlarged to show the sharpness of the reflections. Before each exposure was taken, the beam stop was removed for a few second so that the direct beam is seen in the middle of the equator as a black circle. The light line through this circle is due to absorption by the specimen and glass support. In the low-angle patterns the first eight lamellar reflections are visible. In the wide-angle patterns a few of these lamellar meridional reflections are visible above the beam stop, and the arrows point to the wide-angle reflections. All patterns were recorded at room temperature. A and C are from pure DLPC and B is from a 2 : 1 molar ratio of DLPC:cholesterol, all at 50% relative humidity. The wide-angle reflections in C are located on the equator at a spacing of 4.2 Å. D is from pure DPPC at 100% relative humidity. Lines drawn from the 4.2 Å wide-angle reflections to the origin (image of direct beam) make an angle of about 24° with the equator. The wide-angle meridional arcs are due to scattering from the specimen holder. E is from a 2 : 1 molar ratio of DPPC:cholesterol at 70% relative humidity with diffuse wide-angle reflections at 4.5 Å.

For pure phosphatidylcholine in the liquid crystalline state, and for most phosphatidylcholine/cholesterol mixtures, diffuse reflections at 4.5 Å are recorded. For all specimens this reflection was centered on the equator of the X-ray film. Fig. 1E is a wide-angle pattern from DPPC/cholesterol. Although the 4.5 Å reflection is broad, the amount of arcing away from the equator is only a few degrees. This wide angle pattern remains constant for relative humidities ranging from 50 to 100%. Below 50% humidity, the DPPC and cholesterol often phase separate as two distinct series of lamellar reflections are recorded. The 4.5 Å reflection is slightly broader and more arced for pure phosphatidylcholine in the liquid crystalline state than for the phosphatidylcholine/cholesterol mixtures.

For DLPC/cholesterol, DMPC/cholesterol, and DPPC/cholesterol the wide-angle patterns remain constant (Fig. 1E) over a wide range of relative humidities and temperatures, both above and below the pure lipids' transition temperatures. However, the DSPC/cholesterol wide-angle pattern is considerably different. At room temperature, for all hydration states, there is a broad 4.2 Å reflection oriented on the equator. As the temperature of a fully hydrated specimen is raised, this 4.2 Å reflection remains constant until several degrees below the DSPC phase transition temperature. The reflection then broadens and changes to a diffuse 4.5 Å reflection above the DSPC transition temperature which occurs at 58°C [24].

To calculate the electron density distributions across the various bilayers, it is necessary to determine the sign or phase of each lamellar reflection. Phase determination has previously been described in the case of DPPC [13,25] and egg phosphatidylcholine/cholesterol [15] bilayers. One of the most reliable methods to find phase information for bilayer systems is to determine the continuous Fourier transform of the structure by swelling experiments designed to increase the fluid spaces between bilayers while leaving the bilayers themselves unchanged [15,26—28]. Notice that pure synthetic phosphatidylcholine bilayers cannot be used for swelling experiments since the structure, namely the hydrocarbon chain tilt, changes as water is added to the multilayers. However, phosphatidylcholine/cholesterol bilayers have nearly the same hydrocarbon chain structure over a range of water contents (Fig. 1E). Thus, phosphatidylcholine/cholesterol bilayers can be phased by swelling experiments. In this paper 2 : 1 molar ratios of phosphatidylcholine to cholesterol were used and diffraction patterns were recorded at relative humidities ranging from 50 to 100%. Intensities from diffraction patterns with different repeat periods were put on the same relative scale by the method of Worthington and Blaurock [29] and the correct phase choice was determined by use of the Sampling Theorem [27,30]. For each possible phase combination, $T(h = 0)$ was estimated by the method of King and Worthington [31] and the continuous transforms reconstructed by Sayre's application of the Sampling Theorem [32]. The absolute value of each of these transforms was then compared to all data sets. Only two phase combinations, the correct choice and the extact opposite combination, provided continuous transforms consistent with all data sets. From these remaining two possibilities, the correct choice was determined by assuming that the central hydrocarbon region of the bilayer has a lower electron density than the phospholipid head groups. Continuous transforms for

2 : 1 molar ratios of DLPC/cholesterol and DPPC/cholesterol are shown in Figs. 2 and 3, respectively. The transform in Fig. 2 extends further in reciprocal space and, in general, the shorter chain length lipids give the highest resolution diffraction patterns. Diffraction patterns from pure phosphatidylcholine bilayers (Fig. 1A) are very similar to those of phosphatidylcholine/cholesterol bilayers (Fig. 1B) with small changes in intensity distribution. Thus, the phase choices for the pure phosphatidylcholine bilayers are easily obtainable from the phosphatidylcholine/cholesterol data.

Electron density profiles for the saturated phosphatidylcholines and phosphatidylcholine/cholesterol combinations are shown in Figs. 4—8. There are certain similarities in all the profiles. In all cases the region of lowest electron density is located in the center of the bilayer. This relatively deep and narrow low density trough corresponds to the terminal methyl groups of the hydrocarbon [33]. This central trough is surrounded on either side by a medium density region which represents the methylene groups of the lipid hydrocarbon chains. The high electron density peaks at the edge of each bilayer correspond to the phospholipid head groups. Although all of the profiles have these same general characteristics, the widths, shapes, and relative densities of these terminal methyl, hydrocarbon chain, and head group regions vary according to the chemical composition and physical state of each bilayer.

Fig. 4 shows the difference in structure between a saturated lipid in the gel and liquid crystalline states. DLPC was chosen for this particular study since the highest resolution diffraction patterns for both states were obtained with this lipid. Although fully hydrated DLPC is in the liquid crystalline state at room temperature, DLPC bilayers at room temperature and relative humidities lower than 50% are in the gel state, as determined by wide-angle diffraction (Fig. 1C). An electron density profile of DLPC at low water content in the gel

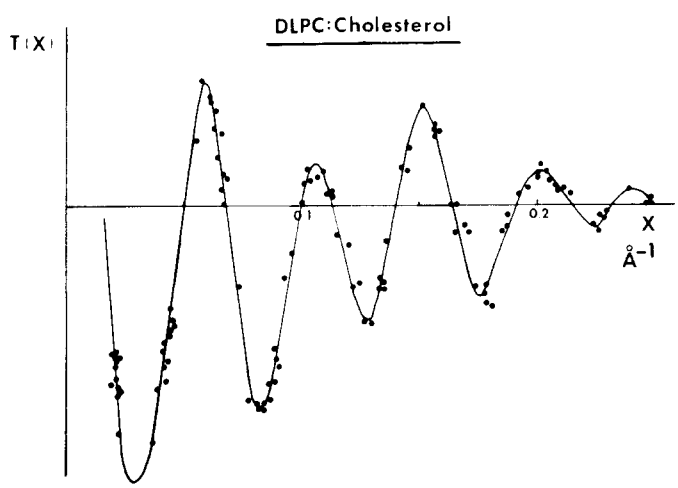

Fig. 2. Structure factors $T(X = h/d)$ of bilayers with a 2 : 1 molar ratio of DLPC:cholesterol from swelling experiments with relative humidities varying from 40 to 100% at $T = 20^{\circ}C$. A total of 12 data sets are included, with the first 10 or 11 orders of diffraction plotted for each set. Repeat periods range from $d = 44$ Å to $d = 54$ Å. The fact that all data points fall on the same curve indicates that the structure of these bilayers is the same throughout this humidity range.

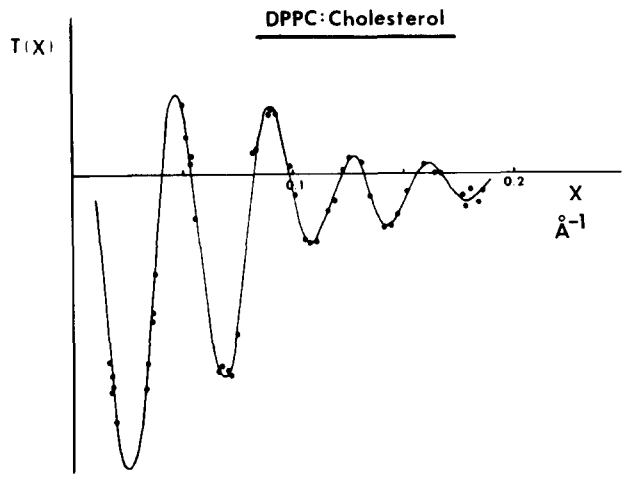

Fig. 3. Structure factors $T(X = h/d)$ for a series of swelling experiments with relative humidities ranging from 50 to 100% for bilayers of 2 : 1 molar ratio DPPC:cholesterol. A total of five data sets are included, with the first 9—11 orders of diffraction plotted for each set. Repeat periods range from 54 to 61 Å. Since all data points fall on the same curve, the structure of these DPPC/cholesterol bilayers is the same throughout this humidity range.

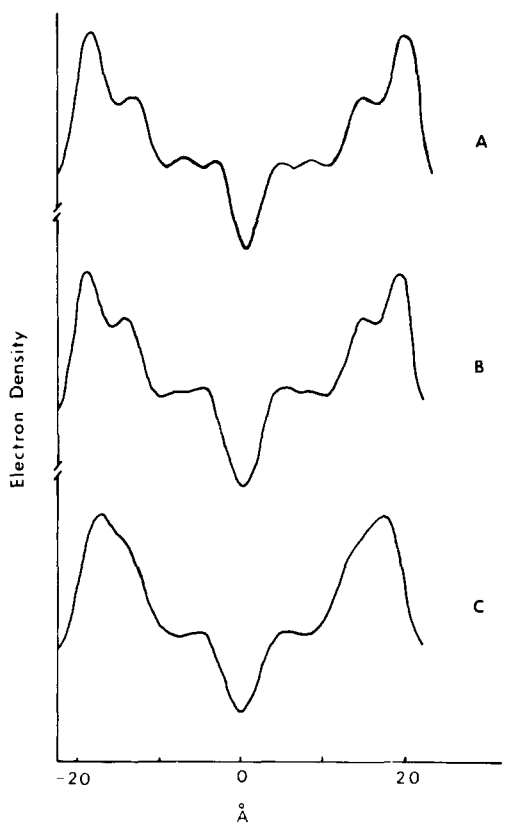

Fig. 4. Electron density profiles of DLPC in the (A) gel state, $T = 20^{\circ}C$, 50% relative humidity, (B) liquid crystalline state, $T = 40^{\circ}C$, 50% relative humidity, and (C) liquid crystalline state at higher water content, $T = 20^{\circ}C$, 75% relative humidity.

state is shown in Fig. 4A. Each head group region contains two characteristic bumps. The outer, higher density bump corresponds to the high density phosphate group, whereas the inner lower density peak corresponds to the glycerol backbone of the head group [34]. It is important to note that the phosphate group peak is located within 5 Å of the edge of the bilayer, implying that the head group cannot be fully extended (see Discussion). The profile of Fig. 4B is of DLPC in the liquid crystalline state at low water content. The total width of this bilayer is about 1 Å less than the bilayer of Fig. 4A. However, the terminal methyl trough is broader by about 1 Å than the DLPC profile in the gel state. DLPC in the liquid crystalline state at higher water content is shown in Fig. 4C. This bilayer is about 3 Å narrower than in the gel state with a broader and shallower methyl trough. In addition, the head group region consists of a single broad peak rather than two distinct bumps. Increased disorder in the head group region is probably the major reason the two distinct peaks smear into a single broad peak. Additional water penetrating into the head group region up to the glycerol backbone would also tend to smear the head group peaks. Thus, although the difference in wide-angle patterns between gel and liquid crystalline states is marked, the differences in electron density profiles are subtle. On going from the gel to liquid crystalline states the total width of the bilayer decreases, while the width of the terminal methyl trough increases, indicating more disorder and less localization of methyl groups in the center of the bilayer in the liquid crystalline state. The amount of disorder in the center of the bilayer increases with increasing water content in the multilayers.

The addition of cholesterol to the bilayer has several effects on the electron density profile. In Fig. 5 profiles of DLPC/cholesterol and pure DLPC in the liquid crystalline state are superimposed. The DLPC/cholesterol profile was

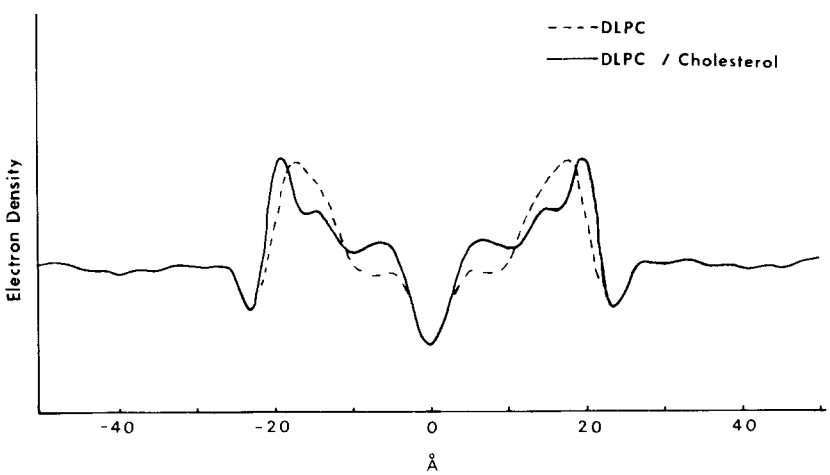

Fig. 5. Electron density distribution of bilayers of pure DLPC in the liquid crystalline state (T = 20°C, 75% relative humidity) and a 2 : 1 molar ratio DPLC:cholesterol derived from the continuous transform data. The presence of cholesterol raises the electron density of the hydrocarbon chain region of the profile adjacent to the head group and also increases the width of the bilayer as it reduces the allowed conformation of the lipid alkyl chains.

generated from the continuous transform of Fig. 2 by selecting structure factors from the curve at an invented repeat period of $d = 100$ Å for the Fourier synthesis calculation. This procedure minimizes Fourier truncation artifacts, clearly displays the relative density of the fluid layers between bilayers, and also provides a check on the phase determination. The correct phase combination provides flat, featureless density layers outside the bilayer, while incorrect phase choices give much larger density fluctuations in these regions. The profiles of Fig. 5 clearly show the effects of cholesterol on DLPC bilayer organization. The width of the bilayer is increased compared to DLPC in the liquid crystalline state, as the cholesterol reduces the allowed conformations of the phospholipid chains, increasing the number of trans conformations [3]. The width of the DLPC/cholesterol bilayer is the same as pure DLPC in the gel state (Fig. 4A). Cholesterol also introduces a marked increase in density in the hydrocarbon chain region of the bilayer, but has little effect on the terminal methyl trough.

Fig. 6 shows the effect of hydration of phosphatidylcholine bilayers, in this case DPPC, below the phase transition temperature. The top profile is the case

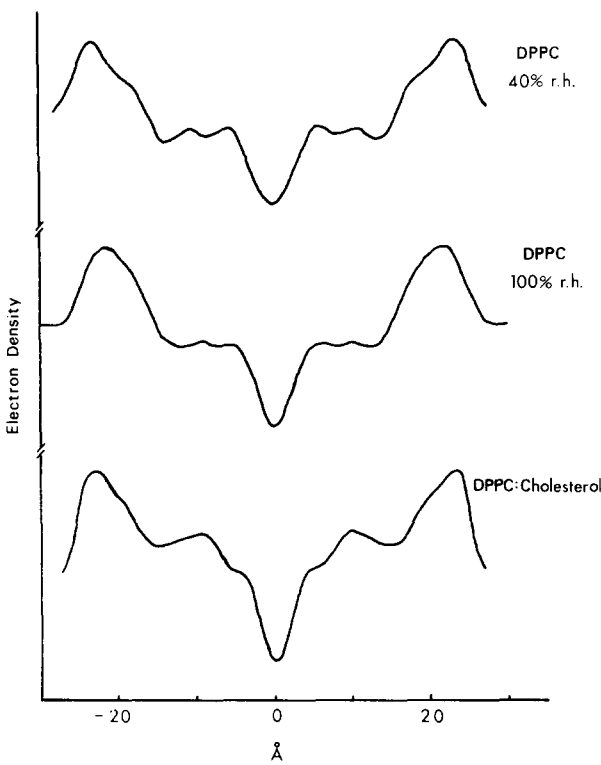

Fig. 6. Electron density distributions across bilayers of pure DPPC in the gel state at 40 and 100% relative humidities and of a 2 : 1 molar ratio DPPC:cholesterol bilayer at 66% relative humidity all at $T = 20^{\circ}C$. The cholesterol steroid rings introduce elevations in the electron density of the hydrocarbon chain region adjacent to the lipid head group. The width of the pure DPPC bilayer changes in different relative humidity atmospheres, as the chain tilt of the lipid molecules change. The width of the DPPC/cholesterol bilayer is the same in all humidities, and is approximately equal to the width of the pure DPPC bilayer when there is no chain tilt.

where the multilayer has low water content and the chains are fully extended perpendicular to the plane of the bilayer. Again, each head group region contains two bumps, corresponding to the phosphate group and glycerol backbone of phosphatidylcholine. This top profile of Fig. 6 is very similar to the ones derived by Lesslauer et al. [13] and by Luzzati et al. [25]. The profile of DPPC at 100% relative humidity (Fig. 6, middle) is different in several ways from the low water content profile. The head group region now consists of a single broad peak, rather than two distinct bumps, and there is a uniform density fluid layer outside the head group region. However, the width of the bilayer, as measured by head group-to-head group separation, has decreased due to the chain tilt (Fig. 1D) introduced by the addition of more water to the multilayers. Notice that the addition of water to phosphatidylcholine bilayers, both in the gel (Fig. 6) and in the liquid crystalline state (Fig. 4), has the effect of changing the profile of the head group from two distinct bumps to a single broad peak.

The addition of the cholesterol to the DPPC bilayer has several effects on the electron density profile (Fig. 6, bottom). The width of the DPPC/cholesterol bilayer is about the same as the pure DPPC bilayer at 40% relative humidity, as cholesterol straightens the hydrocarbon chains for all water contents of the multilayers. There is also the elevated density in the hydrocarbon region of the DPPC/cholesterol bilayer, extending from the head group region in toward the center of the bilayer by about 10 Å. The DPPC/cholesterol profile of Fig. 6 resembles the one derived by Franks [15] for egg phosphatidylcholine/cholesterol and also has similarities in the hydrocarbon chain region to the profile derived for sphingomyelin/cholesterol bilayers by Khare and Worthington [35]. Again, for a more direct indication of the effect of cholesterol on bilayer structure, profiles of DPPC/cholesterol and pure DPPC at 100% relative humidity are superimposed in Fig. 7. The profiles were put on the same relative electron density scale by superimposing the respective fluid layers and centers

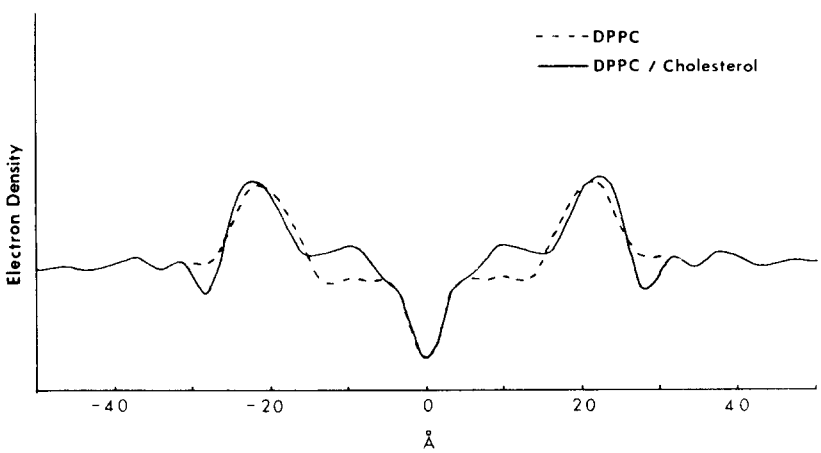

Fig. 7. Electron density distributions of bilayers of pure DPPC at 100% relative humidity in the gel state at $T = 20^{\circ}C$ and 2 : 1 molar ratio DPPC:cholesterol derived from continuous transform data. The presence of cholesterol raises the electron density of the hydrocarbon chain region adjacent to the lipid head group and increases the width of the bilayer by reducing hydrocarbon chain tilt.

of the terminal methyl troughs of the two profiles. The increase in density in the hydrocarbon chain region next to the head group is easily seen in the DPPC/cholesterol bilayer, as is the increase in the width of the bilayer due to the elimination of chain tilt.

Finally, Fig. 8 compares the profile of DSPC/cholesterol and pure DSPC. Again cholesterol introduces an elevation in density in the hydrocarbon chain region. However, in this case the DSPC/cholesterol bilayer is narrower than the pure DSPC bilayer at low water content. The reason for this is that cholesterol is significantly shorter than DSPC, so in the DSPC/cholesterol bilayers the phospholipid hydrocarbon chains tend to kink and bend so that there will not be an empty space in the center of the bilayer. This kinking decreases the width of the bilayer. When the temperature is below the DSPC phase transition temperature, there is a region of gel state lipid hydrocarbon chains in the center of the bilayer. The wide-angle pattern of DSPC/cholesterol consists of a broad 4.2 Å reflection, meaning that some portions of the lipid chains are packed in a hexagonal array, yet with more chain disorder than in pure DSPC bilayers which produce a sharp 4.2 Å reflection.

The DSPC/cholesterol bilayer is wider than fully hydrated pure DSPC bilayer in the gel or liquid crystalline state. In these cases there are two opposing effects on bilayer width. The ends of the phospholipid chains kink to accomodate cholesterol, yet at the same time cholesterol eliminates chain tilt from the fully hydrated gel state DSPC and reduces the allowed conformations of the hydrocarbon chains near the head group for DSPC in the liquid crystalline state.

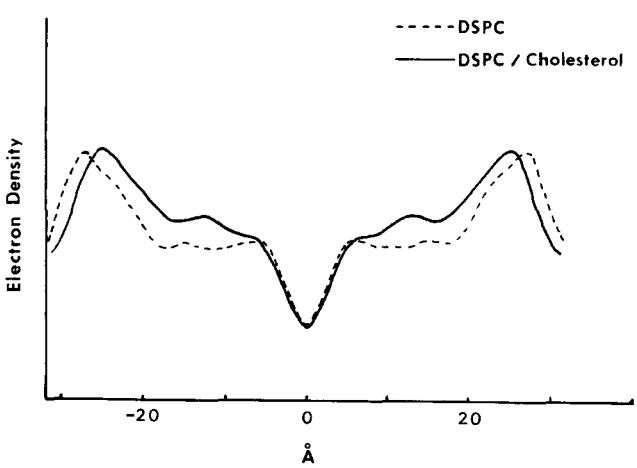

Fig. 8. Electron density distributions of bilayers of pure DSPC and 2 : 1 molar ratio DSPC:cholesterol both at $T = 20^{\circ}C$ and 70% relative humidity. The presence of cholesterol again raises the density of the hydrocarbon chain region adjacent to the head group, but in this instance decreases the total width of the bilayer as the DSPC hydrocarbon chains deform or kink to accomodate the shorther cholesterol molecule.

Discussion

The electron density profiles of Figs. 4—8 clearly localize cholesterol in the bilayer. The steroid rings of cholesterol have sufficiently greater electron density than lipid alkyl chains that they elevate the electron density of the hydrocarbon chain regions of the profiles. Whether the cholesterol is in bilayers of DLPC (Fig. 5), DPPC (Fig. 7), or DSPC (Fig. 8), the elevations in electron density extend from the head group region in about 10 Å toward the center of the bilayer (Fig. 9). Since the distance between the midpoint of the C-OH bond and hydrocarbon tail region of the cholesterol molecule is about 11 Å [36], and since the wide-angle patterns indicate that the lipid hydrocarbon chains are oriented, on the average, perpendicular to the plane of the bilayer, the profiles show that the long axis of the cholesterol aligns itself parallel to the phospholipid alkyl chains. The hydroxyl group of cholesterol must be in very close proximity to the carbonyl group of the phospholipid, as also indicated by several other studies [9,15,37—39]. Regardless of the chain length of the phospholipids, from 12 to 18 carbons, the cholesterol ring groups are located in the same region of the bilayer.

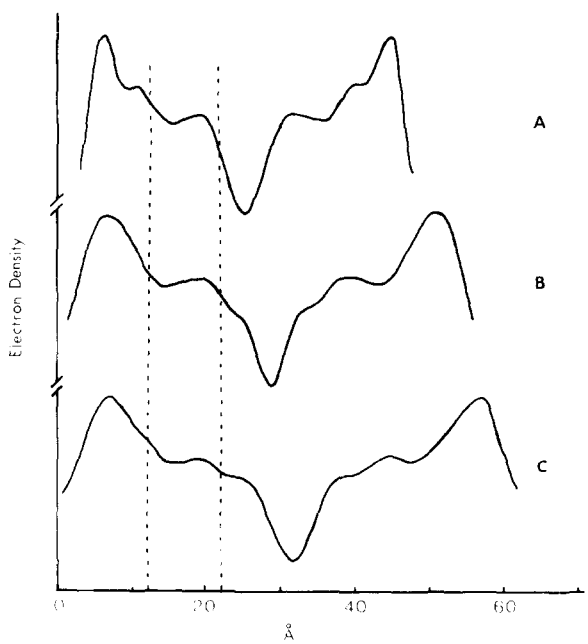

Fig. 9. Electron density profiles of (A) DLPC/cholesterol, (B) DPPC/cholesterol, and (C) DSPC/cholesterol as in Figs. 5, 7, and 8. Origin has been shifted to the edge of the unit cell of DSPC/cholesterol and the head group regions of the three bilayers have been aligned in vertical register. The two dotted lines delimit the evaluations in electron density caused by the cholesterol sterol rings. These elevations are the same distance from the head group region in all cases. The conformationally flexible cholesterol hydrocarbon tail extends from the rings toward the center of the bilayer between approx. 4 and 7 Å. Thus, the cholesterol tail reaches the center of the bilayer in the case of DLPC and comes within 0—3 Å of the center of the bilayer of DPPC. However, there is a 3—6 Å region of pure DSPC chains between the end of the cholesterol tail and the center of the DSPC/cholesterol bilayer.

The hydrocarbon tail of cholesterol provides insufficient contrast from the phospholipid hydrocarbon chains to produce elevations in electron density in the methylene chain region of the bilayer profile. However, the low density terminal methyl ends of lipid molecules can serve as markers, as has been shown for bilayers of mixed chain length fatty acids [40]. In that case, the terminal methyl ends of each fatty acid molecule could be localized by the considerable broadening or repositioning of the methyl trough of the profile (see Fig. 4 of ref. 40). For both the DLPC/cholesterol (Fig. 5) and DPPC/cholesterol bilayers (Fig. 7) there is no broadening of the terminal methyl dip as compared to the pure lipids. In the DLPC/cholesterol profile the higher density steroid ring extends almost to the terminal methyl dip, while in the DPPC/cholesterol profile a short hydrocarbon chain region separates the steroid ring from the terminal methyl dip. Since the terminal methyl dip is not broadened by the addition of cholesterol in either case, the terminal methyl ends of the cholesterol must be localized near the center of the bilayer to within the resolution limits (5 Å) of the profiles. Low resolution ($\approx$14 Å) neutron scattering data [41] also indicates that the hydrocarbon end of the cholesterol molecule is near the center of DPPC/cholesterol bilayers. The conformationally flexible cholesterol hydrocarbon tail may bend to be accomodated in the DLPC/cholesterol bilayer. In the DSPC/cholesterol profile there is a slight broadening of the terminal methyl dip, but more importantly there is a significant decrease in the total width of the bilayer. In this case, the difference in length between fully extended DSPC and cholesterol is such that the DSPC molecule must kink near its methyl end to fill the void that would be caused by the presence of the bulky steroid. Thus, the total bilayer thickness is decreased. A similar phenomenon has been observed in the case of mixtures of fatty acids with phospholipids by Podo and Blasie [42]. Also, the fact that for DSPC/cholesterol the wide-angle pattern is a broad 4.2 Å reflection, rather than 4.5 Å, indicates that at least some portions of the phospholipid chains in the presence of cholesterol are not packed like liquid crystal phase lipids. The 4.2 Å reflection could arise from a domain of DSPC in the multilayers, but since there is not a 4.5 Å reflection present at all in these 2 : 1 molar ratio preparations, or in 1 : 1 molar ratio DSPC/cholesterol bilayers, it seems more likely that that 4.2 Å reflection arises from the ends of the lipid chains near the center of the bilayer.

Thus, cholesterol can be accomodated into bilayers of saturated phosphatidylcholines varying in chain length from 12 to 18 carbons. In DLPC the cholesterol molecule extends from the phospholipid carbonyl group to the center of the bilayer (Fig. 9). In the longer chained DPPC, cholesterol extends to within a few Angstrom units of the center of the bilayer, and there is probably some kinking in the DPPC chains to accomodate the cholesterol. In DSPC, below the phase transition temperature the hydrocarbon chain of the phospholipid is sufficiently long to extend beyond the cholesterol steroid rings and form a region of gel phase lipid in the center of the bilayer. The effect of cholesterol on bilayer width therefore depends on the nature of the phospholipid. The DLPC/cholesterol bilayer is wider than pure DLPC in the liquid crystalline state (Fig. 5) because cholesterol reduces the allowed conformations of the hydrocarbon chains. The DPPC/cholesterol bilayer (Fig. 7) is wider than

pure fully hydrated DPPC in the gel state because cholesterol acts to remove the hydrocarbon chain tilt. On the other hand, cholesterol reduces the width of DSPC bilayers in the gel state (Fig. 8) at low water content since the longer chain DSPC becomes more kinked to accomodate cholesterol.

Cholesterol also tends to keep the structure of the interior of the bilayer constant over a wide range of temperatures and degrees of hydration as judged by the continuous transform data (Figs. 2 and 3) and by the constant nature of the wide-angle diffraction (Fig. 1E) and electron density profiles. Over similar temperature ranges and hydration states the structure of the pure lipid bilayers changes (Figs. 4 and 6).

The terminal methyl trough in the center of the bilayer gets progressively wider as one goes from profiles of DLPC (Fig. 4) to DMPC (not shown) to DPPC (Fig. 6) to DSPC (Fig. 8) in the gel state at approximately the same resolution. This indicates that disorder in the center of the bilayer increases with increasing chain length.

Because the lipid chain tilt and chemical composition of the bilayers are known, these electron density profiles can be used to determined the head group orientation of the phospholipid. The phosphate group peak in the head group is within 5 Å of the edge of the bilayer (Fig. 4A). This means that the phosphatidylcholine head group cannot be fully extended perpendicular to the plane of the bilayer as in that case the choline moiety would extend 6—8 Å beyond the phosphate group. Space filling molecular models fit the electron density distributions and chain tilt parameters only if the phosphocholine dipole is oriented approximately parallel to the plane of the bilayer.

Although the shape of the head group region of the profile changes, the width of this region varies very little on going from the gel to liquid crystalline state (Fig. 4) or upon the addition of water to the multilayers (Figs. 4 and 6). Therefore the phosphatidylcholine head group must be oriented approximately parallel to the bilayer plane in both gel and liquid crystalline states. The exact shape of the head group region of the profile is a function of physical state of the lipid and degree of hydration. For well-ordered DLPC bilayers at low water content (Fig. 4A), the head group region contains distinct phosphorus and glycerol backbone peaks, There is also a density dip at the outer edge of the bilayer (Fig. 4A, Fig. 5). This dip is probably due mainly to Fourier overshoot or Gibb's phenomenon in the limited resolution Fourier syntheses. However, it also may indicate that at least one of the low density methyls of the trimethyl ammonium moiety is not exactly co-planar with the phosphorus in the phosphatidylcholine head groups. Space filling models show that a methyl group can extend out beyond the phosphate group when the phosphatidylcholine head group is parallel to the bilayer plane. In bilayers with less order, as indicated by broadened terminal methyl troughs, such as hydrated DLPC (Fig. 4C) or longer chained DPPC (Fig. 6) or DSPC (Fig. 8), the two separate head group peaks smear into a single density peak. These changes in head group shape in the profile may indicate slight differences in head group conformation, but are more likely to be a function of the degree of molecular order in the bilayer. Thus, although there have been studies indicating that the phosphatidylcholine head group is oriented perpendicular to the bilayer plane [43—45], this present X-ray investigation agrees with recent work [9,38,46,47] that indicate that for

pure phosphatidylcholine bilayers the head group is oriented approximately parallel to the plane of the bilayer in both gel [46] and liquid crystalline [9,38, 46,47] states.

The presence of cholesterol does not drastically change this head group orientation as the width of the head group regions is the same for profiles of phosphatidylcholine/cholesterol and pure phosphatidcylcholine (Figs. 5, 7 and 8). Brown and Seelig [48] have also recently shown by deuterium and ^{31}P NMR studies that the conformation of the head group in DPPC/cholesterol bilayers is 'very similar' to that found in pure DPPC bilayers.

It should also be noted that in DLPC/cholesterol bilayers the two peaks in the head group region of the profile are present even at 100% relative humidity. Thus, the head group region of DLPC/cholesterol profiles more nearly resembles pure DLPC in the gel state (Fig. 4A) or in the liquid crystal state at low relative humidity (Fig. 4B), while the wide-angle diffraction pattern from the hydrocarbon chains of DLPC/cholesterol bilayers is similar to that of DLPC in the liquid crystalline state at high humidity. Due to its location near the phospholipid carbonyl region, the bulky cholesterol molecule tends to preserve molecular order in the head group region of the bilayer while allowing the lipid hydrocarbon chains near the center of the bilayer chains to assume a liquid crystalline type packing. These X-ray results are in accord with NMR data [49] which indicate that cholesterol causes the greatest restriction in motion in the phosphatidylcholine molecule from the glycerol backbone of the head group to approximately halfway down the hydrocarbon chains.

The orientation of the head group in phosphatidylethanolamine has also been shown to be parallel to the plane of the bilayer in single crystals [50] and in sonicated bilayers [51]. However, the structure of phosphatidylcholine bilayers differs from that of phosphatidylethanolamine, particularly in the interior of the bilayer. The electron density profile of Hitchcock et al. [50] for crystals of 1,2-dilauroyl-DL-phosphatidylethanolamine:acetic acid crystals at 5 Å resolution (see Fig. 5b of ref. 50) shows a considerably broader and shallower terminal methyl dip than the comparable resolution profiles of dilauryl phosphatidylcholine and of the other phosphatidylcholines presented in this paper. This is because the terminal methyl groups of the two alkyl chains of the phospholipid are more nearly in register in the center of the bilayer in the case of phosphatidylcholine than in phosphatidylethanolamine. In dilauryl phosphatidylethanolamine the conformation of the glycerol moiety forces the two terminal methyls to be separated by a distance of about 3.6 Å in the direction of the long axis of the molecule [50]. However, the neutron diffraction studies of Buldt et al. [46] show that for DPPC the fatty acid chains are 'out of the step' by only 1.8 Å.

Acknowledgements

I wish to thank Professor J. David Robertson for support and encouragement during the course of these investigations. I am also grateful to Drs. M.J. Costello, S. Simon, W. Longley and J.K. Blasie for very helpful discussions. This work was supported by grants from the National Institutes of Health (Individual Research Fellowship F32 GM05149 and Program Project Research Grants 5 P01 NS 10299 and 9 P01 GM 23911).

References

1 Chapman, D., Cherry, R.J. Phillips, M.C. and Walker, D.A. (1969) Biochim. Biophys. Acta 183, 458—465
2 Joos, P. and Demel, R.A. (1969) Biochim. Biophys. Acta 183, 447—457
3 Lippert, J.L. and Peticolas, W.L. (1971) Proc. Natl. Acad. Sci. U.S. 68, 1572—1576
4 Ladbrooke, B.D., Williams, R.M. and Chapman, D. (1968) Biochim. Biophys. Acta 150, 333—340
5 Darke, A., Finer, E.G., Flook, A.G. and Phillips, M.C. (1971) FEBS Lett. 18, 326—330
6 Taylor, R.P., Huang, C.-H., Broccoli, A.V. and Leake, L. (1977) Arch. Biochem. Biophys. 183, 83—89
7 Hubbell, W.L. and McConnell, H.M. (1971) J. Am. Chem. Soc. 93, 314—326
8 Oldfield, E. and Chapman, D. (1971) Biochem. Biophys. Res. Commun. 43, 610—616
9 Worcester, D.L. and Franks, N.P. (1976) J. Mol. Biol. 100, 359—378
10 Rand, R.P. and Luzzati, V. (1968) Biophys. J. 8, 125—137
11 Levine, Y.K. and Wilkins, M.H.F. (1971) Nat. New Biol. 230, 69—72
12 Engelman, D.M. and Rothman, J.E. (1972) J. Biol. Chem. 247, 3694—3697
13 Lesslauer, W., Cain, J.E. and Blasie, J.K. (1972) Proc. Natl. Acad. Sci. U.S. 69, 1499—1503
14 Cain, J., Santillan, G. and Blasie, J.K. (1972) in Membrane Research (Fox. F., ed.), Vol. 1, 3—14, Academic Press, New York
15 Franks, N.P. (1976) J. Mol. Biol. 100, 345—358
16 Engelman, D.M. and Rothman, J.E. (1972) J. Biol. Chem. 247, 3694—3697
17 Hinz, M.-J. and Sturtevant, J.M. (1972) J. Biol. Chem. 247, 3697—3700
18 Gershfield, N.L. (1977) Biophys. J. 17, 94a
19 Birrell, G.B. and Griffith, O.H. (1976) Arch. Biochem. Biophys. 172, 455—462
20 Longley, W. and Miller, R. (1975) Rev. Sci. Instrum. 46, 30—32
21 Lipson, H. (1967) in International Tables for X-ray Crystallography (Kasper, J.S. and Lonsdale, K., eds.), Vol. II, pp. 265—270
22 O'Brien, F.E.M. (1948) J. Sci. Instr. 25, 73—76
23 Levine, Y.K. (1973) Prog. Surf. Sci. 3, 279—352
24 Chapman, D., Williams, R.M. and Ladbrooke, B.D. (1967) Chem. Phys. Lipids. 1, 445—475
25 Luzzati, V., Tardieu, A. and Taupin, D. (1972) J. Mol. Biol. 64, 269—286
26 Moody, M.F. (1963) Science 142, 1173—1174
27 Worthington, C.R., King, G.I. and McIntosh, T.J. (1973) Biophys. J. 13, 480—494
28 McIntosh, T.J. and Worthington, C.R. (1974) Biophys. J. 14, 363—386
29 Worthington, C.R. and Blaurock, A.E. (1969) Biophys. J. 9, 970—990
30 Shannon, C.E. (1949) Proc. Inst. Radio. Eng. N.Y. 37, 10—21
31 King, G.I. and Worthington, C.R. (1971) Phys. Lett. 35A, 259—260
32 Sayre, D. (1952) Acta Crystallogr. B 5, 843
33 Lesslauer, W. and Blasie, J.K. (1972) Biophys. J. 12, 175—190
34 Wilkins, M.H.F. (1972) Ann. N.Y. Acad. Sci. 195, 291—292
35 Khare, R.S. and Worthington, C.R. (1977) Mol. Cryst. Liq. Cryst. 38, 195—206
36 Rothman, J.E. and Engelman, D.M. (1972) Nat. New Biol. 237, 42—44
37 Brockerhoff, H. (1974) Lipids 9, 645—650
38 Yeagle, P.L., Hutton, W.C., Huang, C. and Martin, R.B. (1975) Proc. Natl. Acad. Sci. U.S. 72, 3477—3481
39 DeKruijff, B. (1978) Biochim. Biophys. Acta 506, 173—182
40 McIntosh, T.J., Waldbillig, R.C. and Robertson, J.D. (1977) Biochim. Biophys. Acta 466, 209—230
41 Schoenborn, B.P. (1977) Chem. Eng. News. Jan. 24, 31—41
42 Podo, F. and Blasie, J.K. (1976) Biochim. Biophys. Acta 419, 1—18
43 Phillips, M.C., Finer, E.G. and Hauser, H. (1972) Biochim. Biophys. Acta 290, 397—402
44 Jendrasiak, G.L. and Mendible, J.C. (1976) Biochim. Biophys. Acta 424, 149—158
45 Hauser, H., Phillips, M.C., Levine, B.A. and Williams, R.J.P. (1976) Nature 261, 390—394
46 Buldt, G., Gally, H.-U., Seelig, A., Seelig, J. and Zaccai, G. (1978) Nature 271, 182—184
57 Seelig, J., Gally, H.U. and Wohlgemuth, R. (1977) Biochim. Biophys. Acta 467, 109—119
48 Brown, M.F. and Seelig, J. (1978) Biochemistry 17, 381—384
49 Godici, P.E. and Landsberger, F.R. (1975) Biochemistry 14, 3927—3933
50 Hitchcock, P.B., Mason, R., Thomas, K.M. and Shipley, G.G. (1974) Proc. Natl. Acad. Sci. U.S. 71, 3036—3040
51 Seelig, J. and Gally, H.U. (1976) Biochemistry 15, 5199—5204